Article

Nucleotide Excision Repair Pathway Activity Is Inhibited by Airborne Particulate Matter (PM$_{10}$) through XPA Deregulation in Lung Epithelial Cells

Ericka Marel Quezada-Maldonado [1,2], Yolanda I. Chirino [3], María Eugenia Gonsebatt [4], Rocío Morales-Bárcenas [1], Yesennia Sánchez-Pérez [1] and Claudia M. García-Cuellar [1,*]

[1] Subdirección de Investigación Básica, Instituto Nacional de Cancerología, San Fernando No. 22, Tlalpan 14080, Mexico; marelquezada0612@gmail.com (E.M.Q.-M.); mobarobiol@yahoo.com.mx (R.M.-B.); s_yesennia@yahoo.com.mx (Y.S.-P.)

[2] Programa de Doctorado en Ciencias Biomédicas, Universidad Nacional Autónoma de México, Ciudad Universitaria, Coyoacán 04510, Mexico

[3] Unidad de Biomedicina, Facultad de Estudios Superiores Iztacala, Universidad Nacional Autónoma de México, Los Reyes Iztacala, Tlalnepantla de Baz 54090, Mexico; irasemachirino@gmail.com

[4] Departamento de Medicina Genómica y Toxicología Ambiental, Instituto de Investigaciones Biomédicas, Universidad Nacional Autónoma de México, Ciudad Universitaria, Coyoacán 04510, Mexico; mgonsebatt@gmail.com

* Correspondence: garcue57@gmail.com; Tel.: +52-55-3693-5200 (ext. 209)

Abstract: Airborne particulate matter with a diameter size of ≤ 10 μm (PM$_{10}$) is a carcinogen that contains polycyclic aromatic hydrocarbons (PAH), which form PAH–DNA adducts. However, the way in which these adducts are managed by DNA repair pathways in cells exposed to PM$_{10}$ has been partially described. We evaluated the effect of PM$_{10}$ on nucleotide excision repair (NER) activity and on the levels of different proteins of this pathway that eliminate bulky DNA adducts. Our results showed that human lung epithelial cells (A549) exposed to 10 μg/cm^2 of PM$_{10}$ exhibited PAH–DNA adducts as well as an increase in RAD23 and XPD protein levels (first responders in NER). In addition, PM$_{10}$ increased the levels of H4K20me2, a recruitment signal for XPA. However, we observed a decrease in total and phosphorylated XPA (Ser196) and an increase in phosphatase WIP1, aside from the absence of XPA–RPA complex, which participates in DNA-damage removal. Additionally, an NER activity assay demonstrated inhibition of the NER functionality in cells exposed to PM$_{10}$, indicating that XPA alterations led to deficiencies in DNA repair. These results demonstrate that PM$_{10}$ exposure induces an accumulation of DNA damage that is associated with NER inhibition, highlighting the role of PM$_{10}$ as an important contributor to lung cancer.

Keywords: DNA adducts; DNA repair inhibition; nucleotide excision repair pathway; particulate matter; lung cancer

1. Introduction

Outdoor air pollution, specifically particulate matter (PM), has an impact on the incidence and mortality of lung cancer worldwide [1,2]. Epidemiological evidence and research in animal and in vitro models supported the classification of PM as a class 1 carcinogen by the International Agency for Research on Cancer (IARC) [3,4]. PM is divided according to its aerodynamic diameters into PM$_{10}$ (≤ 10 μm), PM$_{2.5}$ (≤ 2.5 μm), and ultrafine particles (UFPs) (≤ 0.1 μm). PM$_{10}$ contains all of the smaller fractions, and all of them are deposited in the respiratory tract during breathing [5–9]. PM$_{10}$ is made up of a variety of metals, such as zinc, copper, and vanadium; biological agents, such as pollen, bacteria, and endotoxins; and polycyclic aromatic hydrocarbons (PAH), including benzo(g)perylene (BghiP), dibenzo(a)anthracene (DBahA), and benzo(a)pyrene (BaP). The composition of

PM_{10} plays an important role in its genotoxic and carcinogenic potential because some of these components modify the DNA [10,11].

There are several studies in which the role of PM_{10} components as mediators in the DNA damage has been demonstrated. For instance, metals can mediate an increase in reactive oxygen species (ROS), which, in turn, leads to the oxidation of DNA [12,13]. In this regard, base excision repair (BER) is the pathway responsible for repairing the oxidative DNA lesions that cause small distortions in the helical structure of DNA, but enzymatic and non-enzymatic antioxidant defense also protects cells from the ROS generation induced by PM_{10} exposure [14,15]. However, some other components of PM_{10}, such as PAH, mediate genotoxic effects through the induction of bulky DNA lesions, mainly BaP, which is biotransformed by cytochrome P450 enzymes in combination with microsomal epoxide hydrolase, leading to the generation of the reactive species benzo(a)pyrene-7,8-diol-9,10-epoxide (BPDE), which can form adducts with DNA (BPDE–DNA) and cause significant distortions in the helical structure of this biomolecule [16–21]. The antioxidant defenses and the BER pathway are insufficient for coping with such distortions. The nucleotide excision repair (NER) pathway, which is composed of more than 30 proteins, acts in the removal of bulky lesions formed in the DNA, including the PAH–DNA adducts, through one of two sub-pathways: the global-genome (GG-NER) pathway or the transcription-coupled (TC-NER) pathway [22,23].

Damage recognition is the first step of the pathway and is carried out by the XPC-RAD23 proteins in GG-NER. Unwinding of the DNA strand is the next step and is performed by the helicases XPD and XPB [22,24]. A DNA damage verification step is carried out by the XPA protein, which is a key scaffold protein required for the verification of lesions and for the recruitment of other NER pathway proteins. Proper binding of XPA to the site of DNA damage depends on histone 4 (H4), which is dimethylated in lysine 20 (H4K20me2) in the presence of bulky DNA lesions [25–27]. Together with RPA, XPA forms the pre-incision complex in damaged DNA, which ensures that lesions are properly excised and thus represents an important rate-limiting step. In the third step, the XPF-ERCC1 complex cleaves the damage at the 5′-DNA strand, whereas the 3′ incision is mediated by the XPG endonucleases; at the end, δ or ε DNA polymerases synthesize the new DNA strand using the undamaged strand as a template [28].

Post-translational modifications regulate DNA repair by modulating some factors of the NER pathway, including XPA [29]. The phosphorylation of XPA at serine residue 196 ($pXPA^{S196}$) by kinase ATR enhances the stability of XPA and is required for the formation of the XPA-RPA protein complex. WIP1 phosphatase catalyzes the dephosphorylation of XPA at S196, thus inactivating this protein and reducing the NER pathway's functionality, which might increase the carcinogenic potential of different compounds that cause DNA damage [30–35]. DNA adducts can modify DNA conformation and deregulate replication and transcription. Therefore, the accumulation of this type of DNA lesion can induce genomic instability, lead to the appearance of mutations, and promote carcinogenic processes [36–38]. In relation to this, alterations in the NER repair system have been described in different types of cancer, including lung neoplasms [39,40]. However, the effect of PM_{10} exposure in the NER pathway remains unclear. The aim of this study was to investigate the deregulation of the RAD23, XPD, XPA, $pXPA^{s196}$, H4k20me2, and WIP1 proteins, which are the main components of NER pathway responsible for the removal of bulky DNA damage, establishing an association with the NER pathway activity in A549 lung epithelial cells exposed to PM_{10} for 24 and 48 h.

2. Results

2.1. PM_{10} Induced the Formation of BPDE–DNA Adducts

PM_{10} exposure for 24 h increased the levels of BPDE–DNA adducts in A549 cells compared with the control group (FC = 2.01 vs. 0.0; $p < 0.05$) (Figure 1). PM_{10} exposure for 48 h showed a further increase in BPDE–DNA adducts (FC = 2.54 vs. 0.0; $p < 0.05$). BaP exposure for 24 h increased the levels of BPDE–DNA adducts in A549 cells compared with

the control group (FC = 2.85 vs. 0.0; $p < 0.05$). BaP exposure for 48 h also showed an increase in BPDE–DNA adducts (FC = 1.30 vs. 0.0; $p < 0.05$). The comparison of the times exhibited a significant decrease in the levels of BPDE–DNA adducts among cells treated with BaP for 48 h compared with that in those treated for 24 h (FC = 1.30 vs. 2.85; $p < 0.05$).
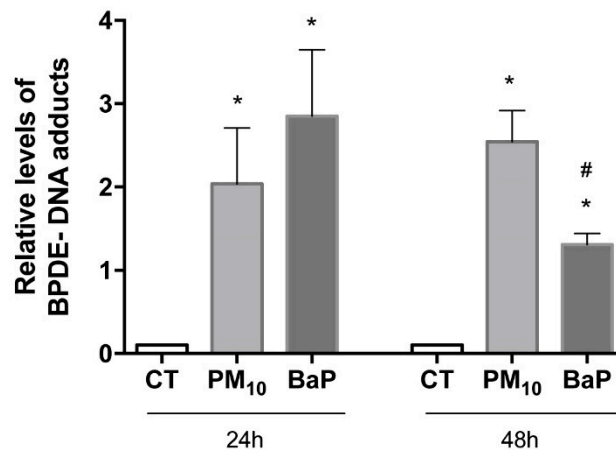

Figure 1. PM_{10} exposure induces the formation of BPDE–DNA adducts in A549 cells. Benzo(a)pyrene diol epoxide-DNA (BPDE–DNA) adducts were evaluated in A549 cells exposed to 10 µg/cm^2 of PM_{10} and 1 µM of BaP for 24 and 48 h. The concentration of BPDE–DNA adducts was measured using the OxiSelect BPDE DNA Adduct ELISA Kit and expressed according to the relative levels, and the values represent results from three experiments with the mean ratio $\pm$ SD per treatment. BaP was used as a positive control for DNA adduct generation. The images are representative of the data obtained. (*) indicates statistical differences versus the control group; $p < 0.05$. (#) indicates statistical differences between the amounts of time; $p < 0.05$.

2.2. PM_{10} Deregulated the RAD23, XPD, and XPA Proteins Used in the Recognition and Verification Step of the NER Pathway

PM_{10} exposure for 6 h increased the RAD23 protein levels in A549 cells compared with the control group (1.16 vs. 1.00; $p < 0.05$) (Figure 2A). BaP exposure for 6 h also increased the RAD23 protein levels compared with the control group (1.20 vs. 1.00; $p < 0.05$). No differences were observed in the RAD23 protein levels after PM_{10} or BaP exposure for 12 h (1.04 and 1.02 vs. 1.00, respectively), 24 h (1.01 and 0.94 vs. 1.00, respectively), or 48 h (0.95 and 0.90 vs. 1.00, respectively) compared with their control groups.

No differences were observed in the XPD protein level after PM_{10} or BaP exposure for 6 h (1.01 and 1.09 vs. 1.00, respectively), 12 h (1.05 and 1.03 vs. 1.00, respectively), or 48 h (0.97 and 0.98 vs. 1.00, respectively) compared with the control groups (Figure 2B). However, PM_{10} exposure for 24 h increased the XPD protein level in A549 cells compared with the control group (1.20 vs. 1.00; $p < 0.05$). BaP exposure for 24 h also increased the XPD protein level compared with the control group (1.15 vs. 1.00; $p < 0.05$).

No differences were observed in the XPA protein level after PM_{10} or BaP exposure for 6 h (1.00 and 0.99 vs. 1.00, respectively), 12 h (1.03 and 1.07 vs. 1.00, respectively), or 48 h (0.98 and 0.96 vs. 1.00, respectively) compared with the control groups (Figure 2C). However, PM_{10} exposure for 24 h decreased the XPA protein level in A549 cells compared with the control group (0.85 vs. 1.00; $p < 0.05$). On the other hand, BaP exposure for 24 h increased the XPA protein level compared with the control group (1.17 vs. 1.00; $p < 0.05$).
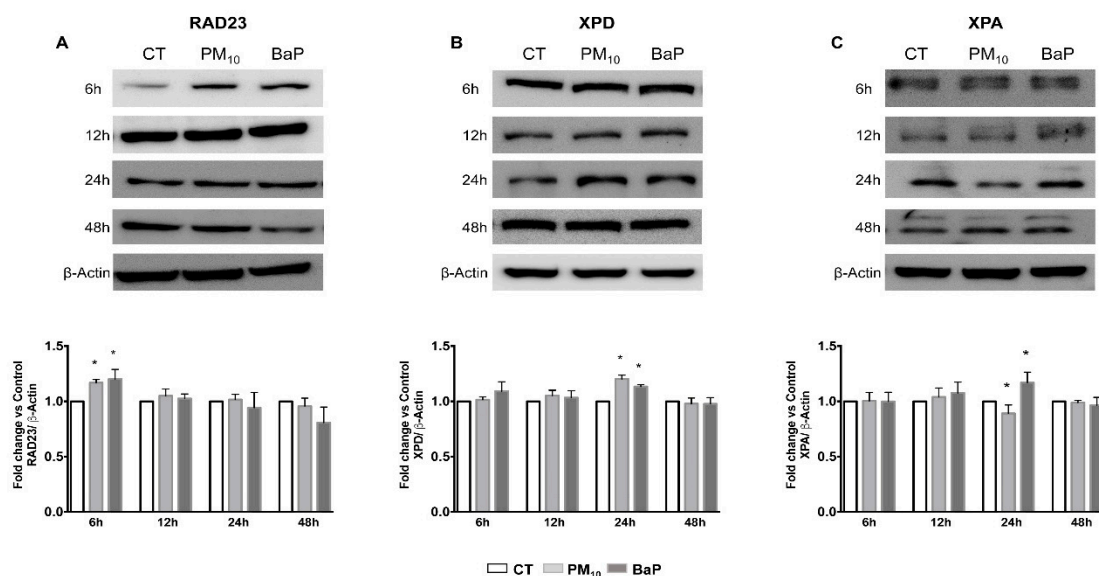
Figure 2. PM$_{10}$ deregulated proteins used in the NER pathway during different stages of exposure in A549 cells. The protein levels of (**A**) RAD23, (**B**) XPD, and (**C**) XPA were evaluated with a Western blot in the total protein lysates of A549 lung epithelial cells exposed to 10 µg/cm^2 of PM$_{10}$ and 1 µM of BaP for 6, 12, 24, and 48 h. Representative images of protein levels in protein lysates (upper panels) and an analysis of densitometry levels (lower panels) using β-Actin as a housekeeping control are shown. β-Actin blot housekeeping control is representative of all time point experiments (see Supplementary Figure S1). The values represent results from three independent experiments with the mean ± SD per treatment. BaP was used as a positive control for NER pathway activation. The images are representative of the data obtained. (*) indicates statistical differences versus the control group; $p < 0.05$.

2.3. PM$_{10}$ Induced Nuclear Recruitment (H4K20me2) and Dephosphorylation of XPA Associated with WIP1 Increase

Cells treated with PM$_{10}$ for 24 h exhibited an increase in nuclear H4K20me2 protein levels compared with the control group (2.09 vs. 1.00; $p < 0.05$), whereas cells treated with BaP for 24 h showed no statistically significant differences (1.10 vs. 1.00) (Figure 3A). In addition, cells treated with PM$_{10}$ for 24 h exhibited a decrease in nuclear pXPA^{S196} protein levels compared with the control group (0.74 vs. 1.00; $p < 0.05$), whereas cells treated with BaP for 24 h showed no differences (1.13 vs. 1.00) (Figure 3B). Interestingly, cells treated with PM$_{10}$ for 24 h exhibited an increase in phosphatase WIP1 protein levels compared with the control group (1.29 vs. 1.00; $p < 0.05$), whereas cells treated with BaP for 24 h showed no differences (1.02 vs. 1.00) (Figure 3C).
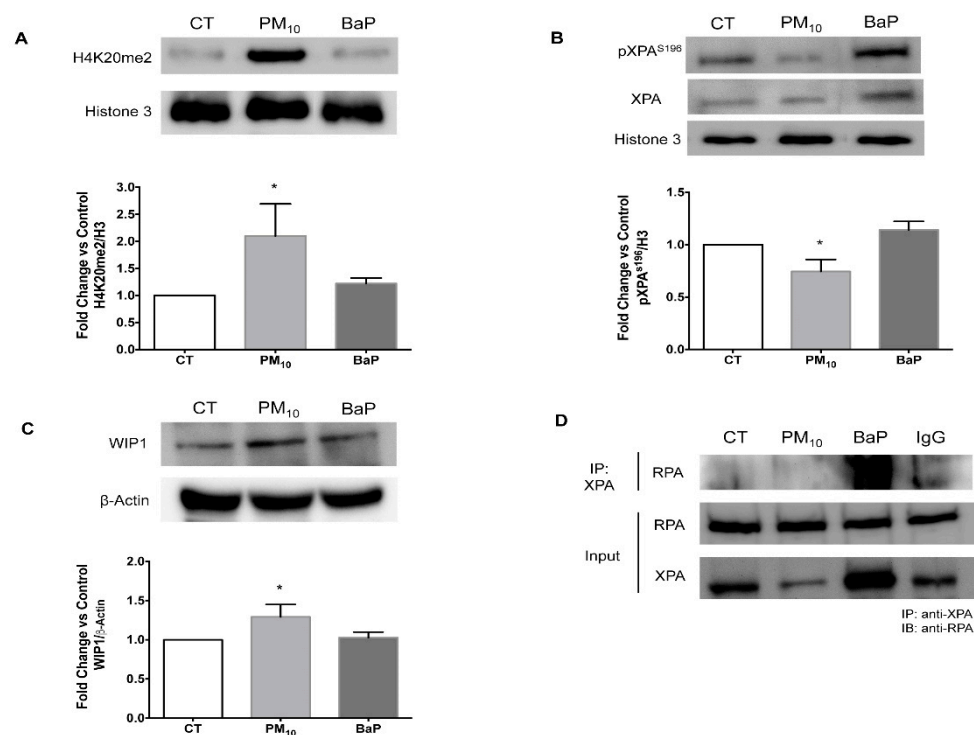
Figure 3. PM_{10} exposure induced signals for the recruitment of XPA into the nucleus but decreased its phosphorylation, thus inhibiting the formation of the XPA-RPA complex in A549 cells. Protein levels were evaluated with a Western blot in nuclear protein lysates of A549 lung epithelial cells after exposure to 10 μg/cm^2 of PM_{10} and 1 μM of BaP for 24 h. BaP was used as a positive control for NER pathway activation. (**A**) Representative Western blot of H4K20me2 in nuclear protein lysates (upper panel) and levels of a densitometry analysis using H3 as an endogenous control (bottom panel). (**B**) Representative Western blot of pXPA^{S196} in cytoplasm and nuclear protein lysates, total XPA is displayed (upper panel) and levels of a densitometry analysis using histone 3 as an endogenous control (bottom panel). (**C**) Representative Western blot of WIP1 levels in total protein lysates (upper panels) and levels of a densitometry analysis using β-Actin as an endogenous control (bottom panels). The images and values represent results from three independent experiments with the mean ± SD per treatment. The images are representative of the data obtained. (*) indicates statistical differences versus the control group; $p < 0.05$. (**D**) Representative Western blot of the interaction between XPA and RPA detected by an immunoprecipitation assay after 24 h. IP: immunoprecipitation, IB: immunoblot. Representative image of three independent experiments.

2.4. PM_{10} Impaired the Formation of the XPA-RPA Complex

Cells treated with PM_{10} for 24 h did not display the XPA-RPA interaction, indicating that the complex between these proteins is not formed, whereas cells treated with BaP for 24 h showed an effective interaction between XPA and RPA, exhibiting a successful formation of this complex (Figure 3D).

2.5. The NER Pathway Was Inactive in Cells Exposed to PM_{10}

Cells treated with PM_{10} for 24 and 48 h showed no differences in NER pathway activity compared with the control groups (0.99 vs. 1.00, and 0.99 vs. 1.00, respectively) (Figure 4). Cells treated with BaP for 24 h showed an increase in NER pathway activity compared with the control group (1.50 vs. 1.00; $p < 0.05$), whereas cells treated with BaP for 48 h showed no differences in NER pathway activity compared with the control group (1.09 vs. 1.00). The comparison between the amounts of time exhibited a significant decrease in NER pathway activity among cells treated with BaP for 48 h compared with those treated for 24 h (1.09 vs. 1.50; $p < 0.05$).
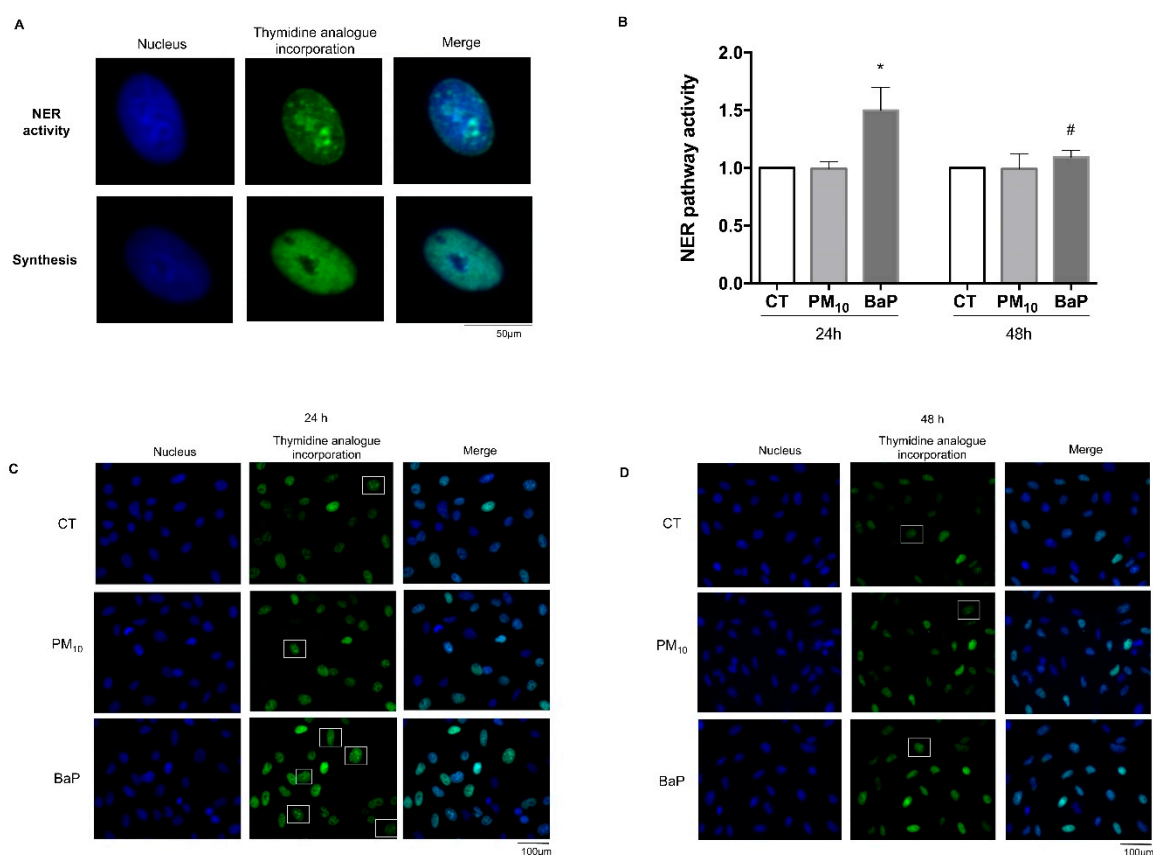
Figure 4. The NER pathway is inactive in A549 cells that are exposed to PM_{10}. The NER pathway's activity was evaluated through unscheduled DNA synthesis (UDS) in A549 lung epithelial cells exposed to 10 μg/cm^2 of PM_{10} and 1 μM of BaP for 24 and 48 h. (**A**) The panel shows representative fluorescence micrographs of the detection of the incorporation of thymidine analog (EdU), and NER pathway activity is recognized according to the formation of foci (upper panel). Non-specific incorporation during DNA synthesis was identified by green homogeneous nucleus staining (lower panel), and these cells were not considered in the cell count for the repair analysis. (**B**) The quantitative results of the NER pathway activity were expressed after counting 1500 cells per condition. The values represent results from three experiments with the mean ratio $\pm$ SD per treatment. BaP was used as a positive control for NER pathway activation. (*) indicates statistical differences versus the control group; $p < 0.05$. (#) indicates statistical differences between the amounts of time compared; $p < 0.05$. (**C**,**D**) Representative images of NER pathway activity (positive cells are marked in white squares) at 24 and 48 h, respectively. The magnification of the NER pathway activity panels can be observed in Supplementary Figure S2 (24 h) and Supplementary Figure S3 (48 h).

3. Discussion

PM_{10} is a well-known risk factor for the development of lung cancer [5,7]. Some of the components of PM_{10} contained in this complex mixture are highly toxic or have been classified as carcinogens, including metals and PAH [17]; however, until now, a mutational fingerprint associated with PM exposure has not been detected [41]. Therefore, the study of the genotoxicity and effects of PM on DNA damage repair pathways could help in understanding the mechanism of PM_{10} in lung carcinogenesis because the evasion of DNA repair induces the accumulation of damaged DNA. It is mainly the altered activity of NER, which is responsible for repairing bulky lesions, that leads to cancer [19,24,42,43]. In this study, A549 cells were exposed to a sub-lethal concentration of 10 μg/cm^2, which simulated human PM_{10} exposure for five days [44,45], and the effects on proteins and the functionality of NER were analyzed.

We showed that PM_{10} induced the formation of BPDE-DNA, and the literature indicated that 60% of bulky lesions are removed within 48 h of their generation [46–48]; however, in cells exposed to PM_{10}, these lesions persisted for over 48 h. By contrast, when the same cell line was exposed to BaP, it showed a decrease in BPDE–DNA adducts at 48 h, suggesting that more than half of the BPDE adducts were eliminated. This highlights that DNA damage induced by PM_{10} could be accumulated more in comparison with the DNA damage induced by BaP, despite being a well-characterized carcinogen. The second main finding of our study is related to a detailed identification of the proteins in the NER pathway. When each step of the repair was evaluated by determining the levels of key NER pathway proteins, we found that in cells exposed to PM_{10}, the RAD23, H4K20me2, and XPD proteins increased, whereas there was a decrease in XPA protein.

NER activity studies have shown that in A549 cells exposed to PAH, the beginning of DNA repair occurs 4 to 6 h after the generation of DNA damage [49]. Therefore, the increase in the RAD23 protein that we observed in cells exposed to PM_{10} in the first hours after exposure suggested that the cells could recognize DNA damage. In addition, in this work, no changes were observed in RAD23 in the following hours of exposure in either PM_{10} or BaP, which indicates that this protein is only necessary during the initial repair step, as has been demonstrated in other studies [26,28,50]. It was also found that after damage recognition, the DNA probably unwinds in cells exposed to PM_{10} because of the increase in the XPD protein, which functions as helicase [27]. Furthermore, PM_{10} increased the levels of H4K20me2, confirming that in cells exposed to PM_{10}, the damaged DNA recognition step works correctly, so this could induce the recruitment of other proteins, such as XPA [25]. In cells exposed to BaP, an increase in XPD levels was found; however, no changes were detected in H4K20me2 levels, so it is likely that this event occurred hours before the protein was measured; further experiments need to be conducted to determine these changes.

Alterations in the XPA protein generate a disruption in the progression of the NER pathway because although XPA does not possess enzymatic activity, it plays a critical role in the assembly of the pre-incision complex in damaged DNA [51]. Importantly, the levels of XPA decrease in cells exposed to PM_{10} even though the recruitment signal for XPA is active, as suggested by the increase in H4K20me2 levels. However, in cells exposed to BaP, an increase in XPA levels was observed, suggesting that in cells exposed to PM_{10}, the verification step is altered. We proposed that the decrease in XPA in cells exposed to PM_{10} could be a consequence of the metals contained in PM_{10} because XPA is structured by zinc fingers [52], and nickel, zinc, cadmium, and copper can oxidize the thiol groups of these domains, thus inducing conformational and structural changes in this protein [48,52–54]. In addition, the reactive oxygen species produced by PM_{10} exposure could also be responsible for alterations in enzymatic activity [55]. We must emphasize that PM_{10} exposure decreased the rate of phosphorylation of XPA, suggesting that PM_{10} alters the function of the XPA protein because dephosphorylated XPA loses its ability to interact with other proteins [33,56]. In addition, altered phosphorylation can lead to a decrease in XPA level, because dephosphorylated XPA is a substrate for HERC2 ubiquitination and proteasome degradation [30,33].

The loss of phosphorylation of XPA in serine 196 observed in this study could be the result of the increase in PM_{10}-induced WIP1 phosphatase levels; Nguyen et al. reported that WIP1 dephosphorylates the serine/threonine residues of different repair proteins, including XPA [31]. In addition, the cells exposed to BaP did not show alterations in either the levels of $pXPA^{S196}$ or WIP1. Cells expressing higher levels of WIP1 have shown reduced repair kinetics for the NER pathway [31,57], and WIP1 overexpression has been reported in some tumors, including lung adenocarcinoma [58,59]. We suggest that PM_{10} exposure could stimulate the phosphatase activity of WIP1 because the functionality of phosphatases depends on low concentrations of metals, such as magnesium or manganese [60,61], and PM_{10} has been shown to contain these metals [18,20]. We propose that the dephosphorylation of XPA induced by exposure to PM_{10} has an impact on the interaction between XPA and RPA because this complex was absent in cells exposed to PM_{10}. Since this complex

performs the verification of damage and recruitment of the excision proteins, such as ERCC1 [51,62,63], we suspect that in cells exposed to PM_{10}, the DNA adducts could not be adequately removed during this step of the NER pathway, in contrast to cells exposed to BaP, which showed a higher rate of DNA adduct removal associated with the presence of the XPA-RPA complex.

Because we observed the persistence of DNA adducts in cells exposed to PM_{10} and we also found alterations in XPA, one of the main proteins of the NER pathway, we decided to measure the activity of the NER pathway. Through this analysis, we confirmed that despite the recognition of damage, the functioning of the NER pathway was inhibited after exposure to PM_{10}. On the contrary, cells exposed to BaP showed a clear increase in the activity of the NER pathway, which is consistent with the decrease in the concentration of BPDE adducts found at 48 h. Therefore, the use of BaP as a positive damage control allowed us to determine that the NER pathway works correctly in A549 cells. The inadequate ability to remove damage indicates that alterations in XPA levels and in the phosphorylation reduce the response of the NER pathway in A549 cells exposed to PM_{10}, highlighting the likely role for WIP1 in inhibition of DNA repair; these are findings that need to be confirmed later. BaP, a carcinogenic component of PM_{10}, had no effect on NER pathway activity, which highlights that the effects on DNA repair activity might be the result of synergistic effects of all PM_{10} components [20].

On the other hand, it is highly likely that NER is not the only DNA repair pathway disrupted by PM_{10} exposure. There is clear evidence of PM_{10}-induced DNA damage, including the detection of 8-hydroxy-2-deoxyguanosine, DNA strand breaks, and formation of γH2AX foci [12,64,65], which is also supported by indirect evidence of DNA damage, such as micronucleus formation [66]; however, the accuracy of the alterations in proteins involved in the DNA repair pathways is still being assessed. For now, some hints of protein dysregulation of the BER pathway, homologous recombination (HR), and nonhomologous end-joining (NHEJ) pathways suggest potential impairment in the global DNA repair after PM_{10} exposure [67]. Together, all DNA repair pathways protect the genome and its fidelity, but according to the literature, deficiencies in the NER and mismatch repair pathways have greater implications for carcinogenesis, whereas alterations in the BER pathway have a very low impact on cancer development [68,69].

Therefore, although additional studies are needed to assess the significance of the results of our study, the data indicate that lung cells exposed to PM_{10} can accumulate DNA damage, which could predispose cells to genomic instability, and, in turn, this could lead to carcinogenesis [70,71]. PM_{10} exposure induces the formation of DNA adducts, and their removal by the NER pathway is impaired in lung epithelial cells so that the risk of lung cancer development attributed to PM_{10} inhalation can be explained by DNA accumulation more than by mutations in early stages of exposure. However, we do not discard that DNA accumulation induced by PM_{10} exposure could lead to mutations that are still not detected (Figure 5).
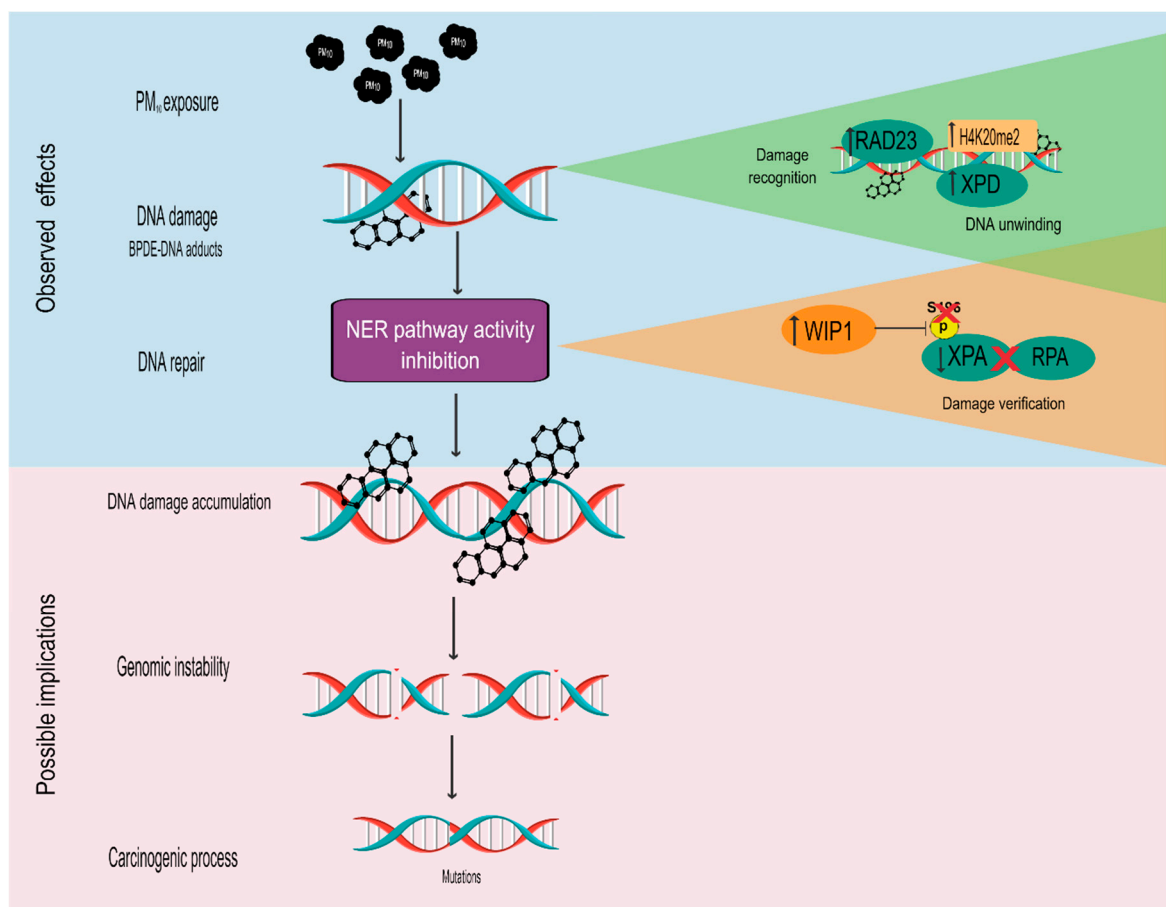
Figure 5. Schematic representation of the possible effects of PM_{10} exposure associated with NER pathway inactivation. Exposure to PM_{10} induces DNA damage through the formation of DNA adducts and this damage is recognized by the overexpression of RAD23, which induces the activity of the XPD and H4K2me2 proteins. Nevertheless, the removal of these adducts is inhibited as a result of the decrease in XPA levels and their dephosphorylation at serine residue 196 mediated by the upregulation of WIP1, which, in turn, disrupts the formation of the complex between XPA and RPA. Therefore, we suggest that the alteration in the functioning of the NER pathway predisposes cells to the accumulation of DNA damage and contributes to genomic instability, which could lead to the generation of mutations and, ultimately, to carcinogenic processes mediated by PM_{10}, which could be aggravated if some other DNA repair pathways are also inactivated.

4. Materials and Methods

4.1. PM_{10} Collection

PM_{10} was collected from a residential urban area of Mexico City, one of the main sources of air pollution in the city, using a high-volume air collector (GMW model 1200 VFC HVPM10 Sierra Andersen, Smyrna, GA, USA) with a constant flow of 1.13 m^3/min. To recover PM_{10}, we used nitrocellulose filters with a pore size of 3.0 μm (Sartorius AG, Goettingen, Germany), which were then scraped with a surgical blade to collect the PM. PM_{10} was stored in endotoxin-free glass vials at 4 °C in the dark until use. The PM_{10} utilized in this study was characterized in previous studies through the analysis of PAH, metals, and endotoxins [72].

4.2. Cell Culture and PM_{10} Exposure

The A549 human lung epithelial cell line was purchased from the American Type Culture Collection (ATCC, Manassas, VA, USA) and was cultured in F-12 Kaighn's medium (Gibco BRL, 21127022, Grand Island, NY, USA) supplemented with 10% heat-inactivated

fetal bovine serum (FBS; GIBCO, 16000044, Life Technologies, Brooklyn, NY, USA) at 37 °C using a 5% CO_2 atmosphere. One milligram of the stock suspension of PM_{10} was resuspended in one milliliter of F-12 Kaighn's medium to obtain a PM_{10} suspension of 1 mg/mL, as previously described [73]. After reaching 70% confluence, cells were exposed to 10 µg/cm^2 of PM_{10} in F-12K medium supplemented with 10% FBS. Cells with only F-12K medium supplemented with 10% FBS were used as a control (CT), and cells treated with BaP (1 µM) (Sigma, B1760, USA) were used as a positive control for DNA adduct generation and the activation of the NER pathway [19,74].

4.3. Measurement of the Benzo(a)pyrene-7,8-diol-9,10-epoxide-DNA Adducts (BPDE-DNA Adduct)

After the cells were exposed to PM_{10} and BaP for 24 or 48 h, DNA was isolated using the phenol–chloroform–isoamyl alcohol extraction protocol of Sambrook et al., 1989 [75]. DNA was dissolved in nuclease-free water and quantified using an ND-1000 spectrophotometer (NanoDrop Technologies, Wilmington, NC, USA). The DNA integrity was evaluated using agarose gel electrophoresis. The BPDE-DNA concentration was measured using the OxiSelect BPDE DNA Adduct ELISA Kit (Cell Bio-labs, Inc., STA-357, San Diego, CA, USA) using the BPDE-DNA standard curve, according to the manufacturer's protocol. The absorbance was read in fluorescence plate reader (Tecan, GENios Plus, Männedorf, Switzerland) at 450 nm. The results were expressed as relative levels represented as fold changes (FCs) based on the calculation of nanograms of BPDE–DNA adducts per microgram of DNA.

4.4. Evaluation of the Total Protein Levels of the NER Pathway

The protein levels of RAD23, XPD, XPA, and WIP1 were evaluated at 6, 12, 24, and 48 h in cells exposed to PM_{10} and BaP. Cells were washed with PBS, and protein extraction was performed using RIPA lysis buffer (20 mM Tris pH 8.0, 1% NP-40, and 150 mM NaCl at pH 8.0) with protease and phosphatase inhibitors (Thermo Fisher, 78440, Rockford, IL, USA). Protein quantification was performed by using the bicinchoninic acid method with a bovine serum albumin curve as a standard (Thermo Fisher, 23209, California, UK). Thirty micrograms of protein were used for electrophoresis on 12% SDS polyacrylamide gels, and the proteins were transferred to 0.45 µm polyvinylidene difluoride (PVDF) membranes using a semidry blotting system (Trans-Blot-Turbo, transfer system; Bio-Rad, California, UK). Membranes were blocked with 5% low-fat milk in TBS-Tween 0.1% under agitation for 1 h. Primary antibodies were incubated in a dilution of 1:1000 (anti-RAD23 cell signaling, 24555, anti-XPD cell signaling, 11963, anti-XPA Santa Cruz, sc-56497, and anti-WIP1 cell signaling, 11901) overnight at 4 °C under constant agitation. Anti-beta-actin (β-Actin) was used as a housekeeping protein in a dilution of 1:3000 (monoclonal antibody donated by Dr. Manuel Hernández, Cinvestav-IPN) [64,76]. After incubation, membranes were washed with TBS–Tween 0.1% and incubated with HRP-secondary anti-rabbit antibody (Amersham, NA934V) 1:2000 or HRP-secondary anti-mouse antibody (Amersham, NA931) 1:3000 for 1 h. Immunodetection was performed with chemiluminescence peroxidase substrate (Millipore, WBKLS0100, Billerica, MA, USA) and with the ChemiDoc-It Imager UVP. A densitometry analysis was performed by using the Image J software.

4.5. Measurements of Nuclear Protein Levels of the NER Pathway

The nuclear protein levels of H4K20me2 and XPA Ser196 were evaluated after the A549 cells were exposed to PM_{10} and BaP for 24 h. Protein extraction was performed by separating the nuclear protein fraction and cytoplasmic protein fraction using Chemicon's nuclear extraction kit (Millipore, 2900, Billerica, MA, USA) according to the manufacturer's instructions. Protein quantification was performed using the bicinchoninic acid assay, as previously mentioned. Fifteen micrograms of nuclear protein fraction was loaded into a 15% SDS-polyacrylamide gel, and the levels of proteins were determined as previously described. Anti-H4K20me2 antibody (Abcam, ab9052) at 1:2000 and anti-phospho-XPA (Ser196) antibody (Thermo Fisher, 64730) at 1:500 were incubated overnight at 4 °C under

constant agitation. Histone 3 (H3) (Abcam, ab1791) was used as a housekeeping protein at 1:5000 for 1 h at room temperature, followed by the incubation of HRP-secondary anti-mouse antibody (Amersham, NA931).

4.6. Detection of the XPA-RPA Protein Complex

The immunoprecipitation assay was performed using the Dynabeads Co-Immunoprecipitation kit (Invitrogen, Thermo Fisher Scientific, 14321D) according to the manufacturer's protocol for detection of the XPA-RPA complex. One milligram of magnetic beads and 5 μg of XPA antibody (Santa Cruz, sc-56497) or 5 μg of normal goat IgG antibody (R&D systems, AB-108-C) were used for the formation of complex ab-magnetic beads. One milligram of protein cell lysates was incubated with the complex ab-magnetic beads. The elution of the immune complex was electrophoresed on 12% SDS-polyacrylamide gel, according to the steps described in the protein determination subsection. Anti-RPA (cell signaling, 2267) antibody at 1:1000 and HRP-secondary anti-rabbit antibody (Amersham, NA934V) at 1:3000 were used.

4.7. Measurement of NER Activity

The activity of the NER pathway was evaluated with an unscheduled DNA synthesis (UDS) assay. This technique provides a direct measurement of the excision and repair of damage after in vitro exposure to the compounds of interest by incorporating the thymidine analogue (5-ethinyl-2'-deoxyuridine (EdU) into DNA during the synthesis of the new strand in the final step of NER [77,78]. DNA replication was blocked (for prevention of nonspecific incorporation of EdU) by incubating the cells with 5 mM hydroxyurea for 2 h before the treatments, and it was left in the culture medium until the end of the corresponding exposure [79]. Subsequently, the cells were exposed to PM_{10} or BaP, and 10 μM EdU was added to the culture medium. After 24 and 48 h of exposure, cells were washed with PBS and fixed using 3.7% paraformaldehyde in PBS for 20 min at room temperature. The incorporation of EdU was visualized with fluorescence microscopy using the Click-iT EdU Imaging Kit (Invitrogen, C10337, Carlsbad, CA, USA) according to the manufacturer's recommendations. At the end of the procedure, the slides were dried, and the nuclei were stained with Prolong Gold antifade DAPI (Invitrogen, 8961S, CA, USA). The UDS slides were observed under an AxioKop2 Mot Plus.D2 fluorescence microscope (Carl Zeiss, Oberkochen, Germany). Micrographs of the different treatments were taken, and the number of EdU-positive cells (foci present in the nucleus) was counted among 1500 cells. Cells that presented a complete staining of their nuclei with EdU (incorporation during the replication of DNA) were excluded from the analysis [78,80] (Figure 4). The activity of the NER pathway was calculated as the percentage of EdU-positive cells in each treatment divided by the percentage of EdU-positive cells present in the control cells.

4.8. Statistical Analysis

The results of at least three independent experiments are presented as means ± standard deviation (SD). Statistical differences between DNA adducts and NER activity were tested by using one way analysis of variance and Bonferroni's post hoc test. Protein levels were tested by applying the two-tailed Student's t-test. All analyses were performed using the GraphPad Software, version 6 and a value of $p \leq 0.05$ was considered statistically significant.

5. Conclusions

Exposure to PM_{10} induces the formation of BPDE–DNA adducts, which are recognizable by RAD23; however, PM_{10} deregulates the damage verification step through the dephosphorylation of XPA at serine 196, thus preventing the formation of the protein complex with RPA, which results in the inhibition of the NER pathway's activity in A549 cells. These findings provide evidence that the impairment of the NER pathway's activity and the damaged DNA might be involved in the carcinogenic potential of airborne particulate

matter, thus helping explain why PM_{10} is considered a risk factor for the development of lung cancer.

References

1. Bai, L.; Shin, S.; Burnett, R.T.; Kwong, J.C.; Hystad, P.; van Donkelaar, A.; Goldberg, M.S.; Lavigne, E.; Weichenthal, S.; Martin, R.V.; et al. Exposure to Ambient Air Pollution and the Incidence of Lung Cancer and Breast Cancer in the Ontario Population Health and Environment Cohort. *Int. J. Cancer* **2020**, *146*, 2450–2459. [CrossRef] [PubMed]
2. Yu, P.; Guo, S.; Xu, R.; Ye, T.; Li, S.; Sim, M.R.; Abramson, M.J.; Guo, Y. Cohort Studies of Long-Term Exposure to Outdoor Particulate Matter and Risks of Cancer: A Systematic Review and Meta-Analysis. *Innovation* **2021**, *2*, 100035. [CrossRef] [PubMed]
3. Loomis, D.; Huang, W.; Chen, G. The International Agency for Research on Cancer (IARC) Evaluation of the Carcinogenicity of Outdoor Air Pollution: Focus on China. *Chin. J. Cancer* **2014**, *33*, 189–196. [CrossRef]
4. Turner, M.C.; Andersen, Z.J.; Baccarelli, A.; Diver, W.R.; Gapstur, S.M.; Pope, C.A.; Prada, D.; Samet, J.; Thurston, G.; Cohen, A. Outdoor Air Pollution and Cancer: An Overview of the Current Evidence and Public Health Recommendations. *CA Cancer J. Clin.* **2020**, *70*, 460–479. [CrossRef] [PubMed]
5. Chen, X.; Zhang, L.-W.; Huang, J.-J.; Song, F.-J.; Zhang, L.-P.; Qian, Z.-M.; Trevathan, E.; Mao, H.-J.; Han, B.; Vaughn, M.; et al. Long-Term Exposure to Urban Air Pollution and Lung Cancer Mortality: A 12-Year Cohort Study in Northern China. *Sci. Total Environ.* **2016**, *571*, 855–861. [CrossRef] [PubMed]
6. Pope, C.A., 3rd; Burnett, R.T.; Thun, M.J.; Calle, E.E.; Krewski, D.; Ito, K.; Thurston, G.D. Lung Cancer, Cardiopulmonary Mortality, and Long-Term Exposure to Fine Particulate Air Pollution. *JAMA* **2002**, *287*, 1132–1141. [CrossRef]
7. Zhou, Y.; Li, L.; Hu, L. Correlation Analysis of PM10 and the Incidence of Lung Cancer in Nanchang, China. *Int. J. Environ. Res. Public Health* **2017**, *14*, 1253. [CrossRef]
8. Moon, D.H.; Kwon, S.O.; Kim, S.-Y.; Kim, W.J. Air Pollution and Incidence of Lung Cancer by Histological Type in Korean Adults: A Korean National Health Insurance Service Health Examinee Cohort Study. *Int. J. Environ. Res. Public Health* **2020**, *17*, 915. [CrossRef]
9. Consonni, D.; Carugno, M.; De Matteis, S.; Nordio, F.; Randi, G.; Bazzano, M.; Caporaso, N.E.; Tucker, M.A.; Bertazzi, P.A.; Pesatori, A.C.; et al. Outdoor Particulate Matter (PM10) Exposure and Lung Cancer Risk in the EAGLE Study. *PLoS ONE* **2018**, *13*, e0203539. [CrossRef]
10. Chen, C.-H.; Wu, C.-D.; Chiang, H.-C.; Chu, D.; Lee, K.-Y.; Lin, W.-Y.; Yeh, J.-I.; Tsai, K.-W.; Guo, Y.L. The Effects of Fine and Coarse Particulate Matter on Lung Function among the Elderly. *Sci. Rep.* **2019**, *9*, 14790. [CrossRef]
11. Yoda, Y.; Takagi, H.; Wakamatsu, J.; Ito, T.; Nakatsubo, R.; Horie, Y.; Hiraki, T.; Shima, M. Stronger Association between Particulate Air Pollution and Pulmonary Function among Healthy Students in Fall than in Spring. *Sci. Total Environ.* **2019**, *675*, 483–489. [CrossRef]
12. Chirino, Y.I.; Sánchez-Pérez, Y.; Osornio-Vargas, Á.R.; Morales-Bárcenas, R.; Gutiérrez-Ruíz, M.C.; Segura-García, Y.; Rosas, I.; Pedraza-Chaverri, J.; García-Cuellar, C.M. PM10 Impairs the Antioxidant Defense System and Exacerbates Oxidative Stress Driven Cell Death. *Toxicol. Lett.* **2010**, *193*, 209–216. [CrossRef]

13. Valavanidis, A.; Vlachogianni, T.; Fiotakis, K. Comparative Study of the Formation of Oxidative Damage Marker 8-Hydroxy-2′-Deoxyguanosine (8-OHdG) Adduct from the Nucleoside 2′-Deoxyguanosine by Transition Metals and Suspensions of Particulate Matter in Relation to Metal Content and Redox Reactivity. *Free Radic. Res.* **2005**, *39*, 1071–1081. [CrossRef]

14. Krokan, H.E.; Bjørås, M. Base Excision Repair. *Cold Spring Harb. Perspect. Biol.* **2013**, *5*, a012583. [CrossRef]

15. Birben, E.; Sahiner, U.M.; Sackesen, C.; Erzurum, S.; Kalayci, O. Oxidative Stress and Antioxidant Defense. *World Allergy Organ. J.* **2012**, *5*, 9–19. [CrossRef]

16. Błaszczyk, E.; Rogula-Kozłowska, W.; Klejnowski, K.; Fulara, I.; Mielżyńska-Švach, D. Polycyclic Aromatic Hydrocarbons Bound to Outdoor and Indoor Airborne Particles (PM2.5) and Their Mutagenicity and Carcinogenicity in Silesian Kindergartens, Poland. *Air Qual. Atmos. Health* **2016**, *10*, 389–400. [CrossRef]

17. Guo, Z.; Wang, Z.; Qian, L.; Zhao, Z.; Zhang, C.; Fu, Y.; Li, J.; Zhang, C.; Lu, B.; Qian, J. Biological and Chemical Compositions of Atmospheric Particulate Matter during Hazardous Haze Days in Beijing. *Environ. Sci. Pollut. Res.* **2018**, *25*, 34540–34549. [CrossRef]

18. Hadei, M.; Aboosaedi, Z.; Naddafi, K. Carcinogenic Risks and Chemical Composition of Particulate Matter Recovered by Two Methods: Wet and Dry Extraction. *Environ. Monit. Assess.* **2020**, *192*, 213–217. [CrossRef]

19. Salcido-Neyoy, M.E.; Sánchez-Pérez, Y.; Osornio-Vargas, A.R.; Gonsebatt, M.E.; Meléndez-Zajgla, J.; Morales-Bárcenas, R.; Petrosyan, P.; Molina-Servin, E.D.; Vega, E.; Manzano-León, N.; et al. Induction of c-Jun by Air Particulate Matter (PM10) of Mexico City: Participation of Polycyclic Aromatic Hydrocarbons. *Environ. Pollut.* **2015**, *203*, 175–182. [CrossRef]

20. Lepers, C.; André, V.; Dergham, M.; Billet, S.; Verdin, A.; Garcon, G.; Dewaele, D.; Cazier, F.; Sichel, F.; Shirali, P. Xenobiotic Metabolism Induction and Bulky DNA Adducts Generated by Particulate Matter Pollution in BEAS-2B Cell Line: Geographical and Seasonal Influence. *J. Appl. Toxicol.* **2013**, *34*, 703–713. [CrossRef]

21. Stiborová, M.; Moserová, M.; Černá, V.; Indra, R.; Dračínský, M.; Šulc, M.; Henderson, C.J.; Wolf, C.R.; Schmeiser, H.H.; Phillips, D.H.; et al. Cytochrome b5 and Epoxide Hydrolase Contribute to Benzo[a]pyrene-DNA Adduct Formation Catalyzed by CytoChrome P450 1A1 under Low NADPH: P450 Oxidoreductase Conditions. *Toxicology* **2014**, *318*, 1–12. [CrossRef]

22. Braithwaite, E.; Wu, X.; Wang, Z. Repair of DNA Lesions Induced by Polycyclic Aromatic Hydrocarbons in Human Cell-Free Extracts: Involvement of Two Excision Repair Mechanisms in Vitro. *Carcinogenesis* **1998**, *19*, 1239–1246. [CrossRef] [PubMed]

23. Butkiewicz, D.; Rusin, M.; Pawlas, M.; Czarny, M.; Chorazy, M. Repair of DNA Damage Using Nucleotide Excision Repair (NER)-Relationship with Cancer Risk. *Postepy Hig. I Med. Dosw.* **2002**, *56*, 485–498.

24. Hoeijmakers, J.H. Nucleotide Excision Repair II: From Yeast to Mammals. *Trends Genet.* **1993**, *9*, 211–217. [CrossRef]

25. Chitale, S.; Richly, H. DICER- and MMSET-Catalyzed H4K20me2 Recruits the Nucleotide Excision Repair Factor XPA to DNA Damage Sites. *J. Cell Biol.* **2017**, *217*, 527–540. [CrossRef]

26. Sugasawa, K.; Ng, J.M.; Masutani, C.; Iwai, S.; van der Spek, P.J.; Eker, A.P.; Hanaoka, F.; Bootsma, D.; Hoeijmakers, J.H. Xeroderma Pigmentosum Group C Protein Complex Is the Initiator of Global Genome Nucleotide Excision Repair. *Mol. Cell* **1998**, *2*, 223–232. [CrossRef]

27. Kuper, J.; Braun, C.; Elias, A.; Michels, G.; Sauer, F.; Schmitt, D.R.; Poterszman, A.; Egly, J.-M.; Kisker, C. In TFIIH, XPD Helicase Is Exclusively Devoted to DNA Repair. *PLoS Biol.* **2014**, *12*, e1001954. [CrossRef]

28. Volker, M.; Moné, M.J.; Karmakar, P.; van Hoffen, A.; Schul, W.; Vermeulen, W.; Hoeijmakers, J.H.; van Driel, R.; van Zeeland, A.A.; Mullenders, L.H. Sequential Assembly of the Nucleotide Excision Repair Factors In Vivo. *Mol. Cell* **2001**, *8*, 213–224. [CrossRef]

29. Rechkunova, N.I.; Maltseva, E.A.; Lavrik, O.I. Post-Translational Modifications of Nucleotide Excision Repair Proteins and Their Role in the DNA Repair. *Biochemistry* **2019**, *84*, 1008–1020. [CrossRef]

30. Lee, T.-H.; Park, J.-M.; Leem, S.-H.; Kang, T.-H. Coordinated Regulation of XPA Stability by ATR and HERC2 during Nucleotide Excision Repair. *Oncogene* **2012**, *33*, 19–25. [CrossRef]

31. Nguyen, T.-A.; Slattery, S.D.; Moon, S.-H.; Darlington, Y.F.; Lu, X.; Donehower, L.A. The Oncogenic Phosphatase WIP1 Negatively Regulates Nucleotide Excision Repair. *DNA Repair* **2010**, *9*, 813–823. [CrossRef]

32. Park, J.-M.; Kang, T.-H. Transcriptional and Posttranslational Regulation of Nucleotide Excision Repair: The Guardian of the Genome against Ultraviolet Radiation. *Int. J. Mol. Sci.* **2016**, *17*, 1840. [CrossRef] [PubMed]

33. Shell, S.M.; Li, Z.; Shkriabai, N.; Kvaratskhelia, M.; Brosey, C.; Serrano, M.; Chazin, W.J.; Musich, P.; Zou, Y. Checkpoint Kinase ATR Promotes Nucleotide Excision Repair of UV-induced DNA Damage via Physical Interaction with Xeroderma Pigmentosum Group A. *J. Biol. Chem.* **2009**, *284*, 24213–24222. [CrossRef] [PubMed]

34. Li, L.; Lu, X.; Peterson, C.A.; Legerski, R.J. An Interaction between the DNA Repair Factor XPA and Replication Protein A Appears Essential for Nucleotide Excision Repair. *Mol. Cell. Biol.* **1995**, *15*, 5396–5402. [CrossRef] [PubMed]

35. Borszéková Pulzová, L.; Ward, T.A.; Chovanec, M. XPA: DNA Repair Protein of Significant Clinical Importance. *Int. J. Mol. Sci.* **2020**, *21*, 2182. [CrossRef]

36. Bai, H.; Wu, M.; Zhang, H.; Tang, G. Chronic Polycyclic Aromatic Hydrocarbon Exposure Causes DNA Damage and Genomic Instability in Lung Epithelial Cells. *Oncotarget* **2017**, *8*, 79034–79045. [CrossRef]

37. Veglia, F.; Matullo, G.; Vineis, P. Bulky DNA Adducts and Risk of Cancer: A Meta-Analysis. *Cancer Epidemiol. Biomark. Prev.* **2003**, *12*, 157–160.

38. Otteneder, M.; Lutz, W.K. Correlation of DNA Adduct Levels with Tumor Incidence: Carcinogenic Potency of DNA Adducts. *Mutat. Res. Mol. Mech. Mutagen.* **1999**, *424*, 237–247. [CrossRef]

39. Cheng, L.; Spitz, M.R.; Hong, W.K.; Wei, Q. Reduced Expression Levels of Nucleotide Excision Repair Genes in Lung Cancer: A Case-Control Analysis. *Carcinogenesis* **2000**, *21*, 1527–1530. [CrossRef]

40. Ide, F.; Iida, N.; Nakatsuru, Y.; Oda, H.; Tanaka, K.; Ishikawa, T. Mice Deficient in the Nucleotide Excision Repair Gene XPA Have Elevated Sensitivity to Benzo[a]pyrene Induction of Lung Tumors. *Carcinogenesis* **2000**, *21*, 1263–1265.

41. Barnes, J.L.; Zubair, M.; John, K.; Poirier, M.C.; Martin, F.L. Carcinogens and DNA Damage. *Biochem. Soc. Trans.* **2018**, *46*, 1213–1224. [CrossRef]

42. Topinka, J.; Schwarz, L.; Wiebel, F.; Černá, M.; Wolff, T. Genotoxicity of Urban Air Pollutants in the Czech Republic: Part II. DNA Adduct Formation in Mammalian Cells by Extractable Organic Matter. *Mutat. Res. Toxicol. Environ. Mutagen.* **2000**, *469*, 83–93. [CrossRef]

43. Palli, D.; Saieva, C.; Munnia, A.; Peluso, M.; Grechi, D.; Zanna, I.; Caini, S.; Decarli, A.; Sera, F.; Masala, G. DNA Adducts and PM10 Exposure in Traffic-Exposed Workers and Urban Residents from the EPIC-Florence City Study. *Sci. Total Environ.* **2008**, *403*, 105–112. [CrossRef] [PubMed]

44. Li, N.; Hao, M.; Phalen, R.F.; Hinds, W.C.; Nel, A.E. Particulate Air Pollutants and Asthma: A Paradigm for the Role of Oxidative Stress in PM-Induced Adverse Health Effects. *Clin. Immunol.* **2003**, *109*, 250–265. [CrossRef] [PubMed]

45. Ferecatu, I.; Borot, M.-C.; Bossard, C.; Leroux, M.; Boggetto, N.; Marano, F.; Baeza-Squiban, A.; Andreau, K. Polycyclic Aromatic Hydrocarbon Components Contribute to the Mitochondria-Antiapoptotic Effect of Fine Particulate Matter on Human Bronchial Epithelial Cells via the Aryl Hydrocarbon Receptor. *Part. Fibre Toxicol.* **2010**, *7*, 18. [CrossRef] [PubMed]

46. Piberger, A.L.; Krüger, C.T.; Strauch, B.M.; Schneider, B.; Hartwig, A. BPDE-Induced Genotoxicity: Relationship between DNA Adducts, Mutagenicity in the in Vitro PIG-A Assay, and the Transcriptional Response to DNA Damage in TK6 Cells. *Arch. Toxicol.* **2017**, *92*, 541–551. [CrossRef] [PubMed]

47. Grosskopf, C.; Schwerdtle, T.; Mullenders, L.H.F.; Hartwig, A. Antimony Impairs Nucleotide Excision Repair: XPA and XPE as Potential Molecular Targets. *Chem. Res. Toxicol.* **2010**, *23*, 1175–1183. [CrossRef]

48. Schwerdtle, T.; Ebert, F.; Thuy, C.; Richter, C.; Mullenders, L.H.F.; Hartwig, A. Genotoxicity of Soluble and Particulate Cadmium Compounds: Impact on Oxidative DNA Damage and Nucleotide Excision Repair. *Chem. Res. Toxicol.* **2010**, *23*, 432–442. [CrossRef]

49. Shi, Q.; Maas, L.; Veith, C.; Van Schooten, F.J.; Godschalk, R.W. Acidic Cellular Microenvironment Modifies Carcinogen-Induced DNA Damage and Repair. *Arch. Toxicol.* **2016**, *91*, 2425–2441. [CrossRef]

50. Riedl, T.; Hanaoka, F.; Egly, J. The Comings and Goings of Nucleotide Excision Repair Factors on Damaged DNA. *EMBO J.* **2003**, *22*, 5293–5303. [CrossRef]

51. Krasikova, Y.S.; Rechkunova, N.I.; Maltseva, E.A.; Lavrik, O.I. RPA and XPA Interaction with DNA Structures Mimicking Intermediates of the Late Stages in Nucleotide Excision Repair. *PLoS ONE* **2018**, *13*, e0190782. [CrossRef] [PubMed]

52. Hu, J.; Hu, Z.; Zhang, Y.; Gou, X.; Mu, Y.; Wang, L.; Xie, X.-Q. Metal Binding Mediated Conformational Change of XPA Protein: A Potential Cytotoxic Mechanism of Nickel in the Nucleotide Excision Repair. *J. Mol. Model.* **2016**, *22*, 1–19. [CrossRef] [PubMed]

53. Hartwig, A.; Asmuss, M.; Ehleben, I.; Herzer, U.; Kostelac, D.; Pelzer, A.; Schwerdtle, T.; Bürkle, A. Interference by Toxic Metal Ions with DNA Repair Processes and Cell Cycle Control: Molecular Mechanisms. *Environ. Health Perspect.* **2002**, *110* (Suppl. 5), 797–799. [CrossRef] [PubMed]

54. Kopera, E.; Schwerdtle, T.; Hartwig, A.; Bal, W. Co (II) and Cd (II) Substitute for Zn (II) in the Zinc Finger Derived from the DNA Repair Protein XPA, Demonstrating a Variety of Potential Mechanisms of Toxicity. *Chem. Res. Toxicol.* **2004**, *17*, 1452–1458. [CrossRef] [PubMed]

55. Jan, R.; Roy, R.; Bhor, R.; Pai, K.; Satsangi, P.G. Toxicological Screening of Airborne Particulate Matter in Atmosphere of Pune: Reactive Oxygen Species and Cellular Toxicity. *Environ. Pollut.* **2019**, *261*, 113724. [CrossRef] [PubMed]

56. Wu, X.; Shell, S.M.; Yang, Z.; Zou, Y. Phosphorylation of Nucleotide Excision Repair Factor Xeroderma Pigmentosum Group A by Ataxia Telangiectasia Mutated and Rad3-Related–Dependent Checkpoint Pathway Promotes Cell Survival in Response to UV Irradiation. *Cancer Res.* **2006**, *66*, 2997–3005. [CrossRef]

57. Fiscella, M.; Zhang, H.; Fan, S.; Sakaguchi, K.; Shen, S.; Mercer, W.E.; Woude, G.F.V.; O'Connor, P.M.; Appella, E. Wip1, a Novel Human Protein Phosphatase That Is Induced in Response to Ionizing radiation in a p53-Dependent Manner. *Proc. Natl. Acad. Sci. USA* **1997**, *94*, 6048–6053. [CrossRef]

58. Bai, F.; Zhou, H.; Fu, Z.; Xie, J.; Hu, Y.; Nie, S. NF-κB-Induced WIP1 Expression Promotes Colorectal Cancer Cell Proliferation through mTOR Signaling. *Biomed. Pharmacother.* **2018**, *99*, 402–410. [CrossRef]

59. Zhao, M.; Zhang, H.; Zhu, G.; Liang, J.; Chen, N.; Yang, Y.; Liang, X.; Cai, H.; Liu, W. Association between Overexpression of Wip1 and Prognosis of Patients with Non-Small Cell Lung Cancer. *Oncol. Lett.* **2016**, *11*, 2365–2370. [CrossRef]

60. Tanoue, K.; Jenkins, L.M.M.; Durell, S.R.; Debnath, S.; Sakai, H.; Tagad, H.D.; Ishida, K.; Appella, E.; Mazur, S.J. Binding of a Third Metal Ion by the Human Phosphatases PP2Cα and Wip1 Is Required for Phosphatase Activity. *Biochemistry* **2013**, *52*, 5830–5843. [CrossRef]

61. Shi, Y. Serine/Threonine Phosphatases: Mechanism through Structure. *Cell* **2009**, *139*, 468–484. [CrossRef] [PubMed]

62. Yang, Z.-G.; Liu, Y.; Mao, L.Y.; Zhang, J.-T.; Zou, Y. Dimerization of Human XPA and Formation of XPA2−RPA Protein Complex. *Biochemistry* **2002**, *41*, 13012–13020. [CrossRef] [PubMed]

63. Topolska-Woś, A.M.; Sugitani, N.; Cordoba, J.J.; Le Meur, K.V.; Le Meur, R.; Kim, H.S.; Yeo, J.-E.; Rosenberg, D.; Hammel, M.; Schärer, O.D.; et al. A Key Interaction with RPA Orients XPA in NER Complexes. *Nucleic Acids Res.* **2020**, *48*, 2173–2188. [CrossRef]

64. Sánchez-Pérez, Y.; Chirino, Y.I.; Vargas, A.O.; Morales-Bárcenas, R.; Gutierrez-Ruiz, M.C.; Vázquez-López, I.; Garcia-Cuellar, C.M. DNA Damage Response of A549 Cells Treated with Particulate Matter (PM10) of Urban Air Pollutants. *Cancer Lett.* **2009**, *278*, 192–200. [CrossRef]

65. Calderón-Garcidueñas, L.; Herrera-Soto, A.; Jury, N.; Maher, B.A.; González-Maciel, A.; Reynoso-Robles, R.; Ruiz-Rudolph, P.; van Zundert, B.; Varela-Nallar, L. Reduced Repressive Epigenetic Marks, Increased DNA Damage and Alzheimer's Disease Hallmarks in the Brain of Humans and Mice Exposed to Particulate Urban Air Pollution. *Environ. Res.* **2020**, *183*, 109226. [CrossRef] [PubMed]

66. Santibáñez-Andrade, M.; Sánchez-Pérez, Y.; Chirino, Y.I.; Morales-Bárcenas, R.; García-Cuellar, C.M. Long Non-Coding RNA NORAD Upregulation Induced by Airborne Particulate Matter (PM10) Exposure Leads to Aneuploidy in A549 Lung Cells. *Chemosphere* **2020**, *266*, 128994. [CrossRef]

67. Quezada-Maldonado, E.M.; Sánchez-Pérez, Y.; Chirino, Y.I.; García-Cuellar, C.M. Airborne Particulate Matter Induces Oxidative Damage, DNA Adduct Formation and Alterations in DNA Repair Pathways. *Environ. Pollut.* **2021**, *287*, 117313. [CrossRef]

68. Papadopoulos, N.; Lindblom, A. Molecular Basis of HNPCC: Mutations of MMR Genes. *Hum. Mutat.* **1997**, *10*, 89–99. [CrossRef]

69. Yoshioka, K.-I.; Kusumoto-Matsuo, R.; Matsuno, Y.; Ishiai, M. Genomic Instability and Cancer Risk Associated with Erroneous DNA Repair. *Int. J. Mol. Sci.* **2021**, *22*, 12254. [CrossRef]

70. Langie, S.A.S.; Koppen, G.; Desaulniers, D.; Al-Mulla, F.; Altemaimi, R.; Amedei, A.; Azqueta, A.; Bisson, W.H.; Brown, D.; Brunborg, G.; et al. Causes of Genome Instability: The Effect of Low Dose Chemical Exposures in Modern Society. *Carcinogenesis* **2015**, *36*, S61–S88. [CrossRef]

71. Wilhelm, T.; Said, M.; Naim, V. DNA Replication Stress and Chromosomal Instability: Dangerous Liaisons. *Genes* **2020**, *11*, 642. [CrossRef] [PubMed]

72. Chirino, Y.I.; García-Cuellar, C.M.; García-García, C.; Soto-Reyes, E.; Osornio-Vargas, Á.R.; Herrera, L.A.; López-Saavedra, A.; Miranda, J.; Quintana-Belmares, R.; Pérez, I.R.; et al. Airborne Particulate Matter in Vitro Exposure Induces Cytoskeleton Remodeling through Activation of the ROCK-MYPT1-MLC Pathway in A549 Epithelial Lung Cells. *Toxicol. Lett.* **2017**, *272*, 29–37. [CrossRef] [PubMed]

73. Quezada-Maldonado, E.M.; Sánchez-Pérez, Y.; Chirino, Y.I.; Vaca-Paniagua, F.; García-Cuellar, C.M. miRNAs Deregulation in Lung Cells Exposed to Airborne Particulate Matter (PM10) Is Associated with Pathways Deregulated in Lung Tumors. *Environ. Pollut.* **2018**, *241*, 351–358. [CrossRef] [PubMed]

74. Abbas, I.; Garcon, G.; Saint-Georges, F.; Andre, V.; Gosset, P.; Billet, S.; Le Goff, J.; Verdin, A.; Mulliez, P.; Sichel, F.; et al. Polycyclic Aromatic Hydrocarbons within Airborne Particulate Matter (PM2.5) Produced DNA Bulky Stable Adducts in a Human Lung Cell Coculture Model. *J. Appl. Toxicol.* **2011**, *33*, 109–119. [CrossRef]

75. Sambrook, J.; Fritsch, E.R.; Maniatis, T. *Molecular Cloning: A Laboratory Manual*, 2nd ed.; Harbor, C.S., Ed.; Cold Spring Harbor Laboratory Press: Long Island, NY, USA, 1989.

76. Morales-Bárcenas, R.; Chirino, Y.I.; Sánchez-Pérez, Y.; Osornio-Vargas, Á.R.; Melendez-Zajgla, J.; Rosas, I.; García-Cuellar, C.M. Particulate Matter (PM10) Induces Metalloprotease Activity and Invasion in Airway Epithelial Cells. *Toxicol. Lett.* **2015**, *237*, 167–173. [CrossRef]

77. Wienholz, F.; Vermeulen, W.; Marteijn, J.A. Amplification of Unscheduled DNA Synthesis Signal Enables Fluorescence-Based Single Cell Quantification of Transcription-Coupled Nucleotide Excision Repair. *Nucleic Acids Res.* **2017**, *45*, e68. [CrossRef]

78. Peter, F. Guengerich Mechanisms of Drug Toxicity and Relevance to Pharmaceutical Development. *Drug Metab. Pharmacokinet.* **2011**, *26*, 3–14. [CrossRef]

79. Salic, A.; Mitchison, T.J. A Chemical Method for Fast and Sensitive Detection of DNA Synthesis in Vivo. *Proc. Natl. Acad. Sci. USA* **2008**, *105*, 2415–2420. [CrossRef]

80. Bendjennat, M.; Boulaire, J.; Jascur, T.; Brickner, H.; Barbier, V.; Sarasin, A.; Fotedar, A.; Fotedar, R. UV Irradiation Triggers Ubiquitin-Dependent Degradation of p21WAF1 to Promote DNA Repair. *Cell* **2003**, *114*, 599–610. [CrossRef]